Eur. Phys. J. D **41**, 513–517 (2007)
DOI: 10.1140/epjd/e2006-00253-5

**THE EUROPEAN
PHYSICAL JOURNAL D**

Structures and magnetic properties of $\mathbf{Au_nTi_2^+}$ ($\mathbf{n \leqslant 7}$) clusters

M.X. Chen[1,2], X.H. Yan[2,a], and S. Wei[3]

[1] Key Laboratory for Advanced Materials and Rhelogical Properties of Ministry of Education, Institute of Modern Physics, Xiangtan University, Xiangtan 411105, Hunan, P.R. China
[2] College of science, Nanjing University of Aeronautics and Astronautics, Jiangsu-210016, P.R. China
[3] Department of Physics, Fudan University, Shanghai-200433, P.R. China

Received 15 May 2006 / Received in final form 26 September 2006

Abstract. Base on the density-functional theory, the structural and magnetic properties of $\mathrm{Au}_n\mathrm{Ti}_2^+$ ($n \leqslant 7$) clusters are investigated. The two titanium atoms form a dimer in the gold clusters. The second-order energy differences and HOMO-LUMO gap provide a clear explanation of the abundance peaks and odd-even staggering observed recently in photofragmentation experiments. The magnetism of $\mathrm{Au}_n\mathrm{Ti}_2^+$ cluster shows an odd-even effect when n increases from 1 to 4 and drops to zero at $n = 5$ and 7. The local magnetic moment and charge partition of Ti 4*s*, 3*d* orbitals are discussed. The peculiar magnetic properties are related to the structures and the hybridization between the Au 5*d*, 6*s* states and Ti 3*d*, 4*s* states.

PACS. 75.40.Mg Numerical simulation studies – 36.40.Cg Electronic and magnetic properties of clusters – 61.46.Bc Clusters

1 Introduction

Since the electronic shell structure has been observed experimentally in alkali metal clusters, a simple phenomenological model named spherical jellium model [1] in which valence electrons move freely in an effective electrostatic potential provided by ionic cores and the other valence electrons, successfully explained size-dependent features of these clusters. After then, this model has been extended to noble metal clusters [2,3], but it is not suits for transition metal (TM) clusters with an open *d*-shell. The stability of typical transition metal clusters as a function of the cluster size is often discussed in terms of shells of atoms, relating the number of atoms needed to form a compact symmetric structure to an enhanced stability [4]. And the *d* electrons are responsible for most interesting properties of TM doped clusters.

Recently, some interesting works on the highly stable TM doped gold clusters with a large gap between highest occupied molecular orbital (HOMO) and lowest unoccupied molecule orbital (LUMO) have been reported MAu_n for M = Mo and W when $n = 12$ [5,6] or M = Zr and Hf when $n = 14$ [7]. In order to understand the interplay between electronic and geometric effects in bimetallic clusters, Neukermans and co-workers investigated the stability of cationic clusters $\mathrm{Au}_n\mathrm{M}^+$ and $\mathrm{Ag}_n\mathrm{M}^+$ [8–10], with M from Sc to Ni, by means of photofragmentation experiments. The observed intensity shown an enhanced abundance for specific cluster sizes and could be discussed on the basis of the jellium model. Motivated by the experimental progresses, first-principle calculations of $\mathrm{Au}_n\mathrm{M}^+$ (M = Sc, Ti, V, Mn, Fe, Au; $n \leqslant 9$) have been performed [11]. A peculiar magnetism of $\mathrm{Au}_n\mathrm{M}^+$ is observed and found to depend on the interaction between the impurity and host atoms.

More recently, Neukermans et al. have extended investigations to multiply TM atoms doped gold clusters by cationic photofragmentation mass spectrometry [12]. They found that for $\mathrm{Au}_n\mathrm{X}_2^+$ (X = Sc, Ti, Fe, and Cr) the observed enhanced stability can be relate the electronic shell model, but it is not straightforward to count the number of delocalized electrons. Despite success in stability of clusters, however, the fragmentation experiment provides poor information on the other properties such as geometrical and electronic structures. Furthermore it is imperative to investigate the influence of doped TM atoms on structures and electronic properties in the bimetallic clusters. Under this background, we perform spin-density functional calculations for two titanium atoms doped gold clusters, aim at explaining enhanced stability of clusters observed by the experiment and presenting a detailed study of the growth behavior and magnetic properties from a first principles approach.

2 Computational details

Our calculations on the geometric and electronic structures of $\mathrm{Au}_n\mathrm{Ti}_2^+$ ($1 \leqslant n \leqslant 7$) based upon the spin-polarized density functional theory (DFT) using the DMol^3 package [13]. The electron density functional is treated by the generalized gradient approximation (GGA)

---

[a] e-mail: `xhyan@nuaa.edu.cn`

with the exchange-correlation potential parametrized by Perdew and Wang (PW91) [14]. The relativistic effect is significant for gold clusters. A relativistic effective core potential (ECP) and a double numerical basis set together with polarization function are used in the calculations. Geometry optimizations are performed by the Broyden Fletcher Goldfarb Shanno (BFGS) algorithm without any symmetry constraints. Self-consistent-field procedures are done with a convergence criterion of 10^{-3} a.u. on the gradient and displacement, and 10^{-5} a.u. on the total energy and electron density.

3 Results and discussion

3.1 Atomic structures and stability

The ground-state geometries of $\mathrm{Au}_n\mathrm{Ti}_2^+$ (n = 1–7) clusters and typical stable isomers are presented in Figure 1, where the host atoms Au is shown in a dark sphere. The most stable structure of $\mathrm{Au}_n\mathrm{Ti}_2^+$ cluster can be obtained by adding one gold atom to that of $\mathrm{Au}_{n-1}\mathrm{Ti}_2^+$. The geometry of AuTi_2^+ cation in the lowest energy state is an isoceles triangle in which Au atom is at the apex. The lowest energy structure for $\mathrm{Au}_2\mathrm{Ti}_2^+$ being a rhombus can be considered as a gold atom bind to the AuTi_2^+ cluster or substituted two gold atoms with Ti_2 in Au_4^+. The first three-dimensional (3D) structure occurs at $n \geqslant 3$. Three Au atoms form an equilateral triangle cycling the Ti_2 dimer. The most stable structure for $\mathrm{Au}_4\mathrm{Ti}_2^+$ with C_{2V} symmetry can be considered as a gold atom added to that of $\mathrm{Au}_3\mathrm{Ti}_2^+$. By adding a gold atom to the structure of $\mathrm{Au}_4\mathrm{Ti}_2^+$, we get the pentagonal bipyramid of $\mathrm{Au}_5\mathrm{Ti}_2^+$, which is the largest binding energy structure for $\mathrm{Au}_5\mathrm{Ti}_2^+$. The most stable structure of $\mathrm{Au}_6\mathrm{Ti}_2^+$ can be obtained by adding an Au atom to the most stable structure of $\mathrm{Au}_5\mathrm{Ti}_2^+$. While symmetrically adding two Au atoms to the pentagonal bi-pyramid structure, we get lowest energy structure of $\mathrm{Au}_7\mathrm{Ti}_2^+$. In contrary to cationic $\mathrm{Au}_n\mathrm{Ti}$ [10] and Au_n [15–17] ($n \leqslant 6$) clusters favor to planar structures, however, the $\mathrm{Au}_{n-1}\mathrm{Ti}_2^+$ clusters prefer compact structures, similar to those of pure titanium clusters [18]. This indicates that the titanium atoms have a significant effect on the structures.

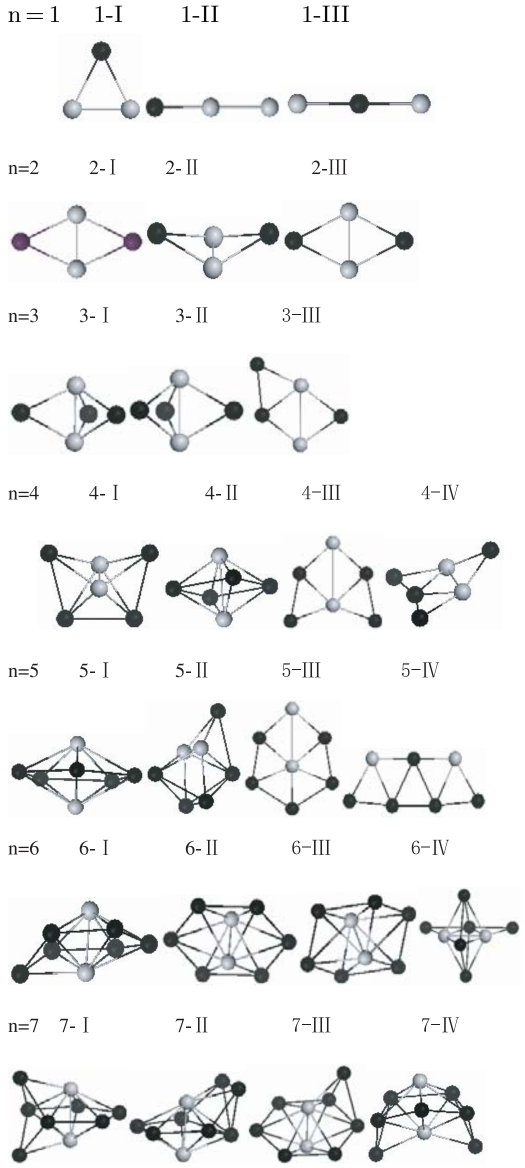

Fig. 1. Equilibrium geometries of the few isomers of cationic $\mathrm{Au}_n\mathrm{Ti}_2^+$ clusters, with $n \leqslant 7$. The gold atoms are represented by dark spheres. The Roman numerals identify each geometry in Table 1.

As a general trend, the two titanium atoms form a dimer in the gold cluster and sit in the center. This is similar to the case of $\mathrm{Au}_8\mathrm{Ti}_2$ clusters [19,20] in which the Au atoms prefer on the surface and the Ti atoms tend to locate in the center. The calculated binding energy of dimers, E_b(Ti–Ti) (2.131 eV) > E_b(Ti–Au) (1.918 eV) > E_b(Au–Au) (1.075 eV). Thus, the two Ti atoms form a dimer and the dimer locates in the center does in favor of stabling the clusters. It is interesting to note that the Ti–Ti distance (Tab. 1) in $\mathrm{Au}_n\mathrm{Ti}_2$ clusters are 2.331 Å, 2.279 Å and 2.307 Å respectively for $n \leqslant 3$, smaller than that of bare cationic titanium dimer with the bond length 2.353 Å. For larger size clusters, the Ti–Ti distance is in the range of 2.370 Å to 2.488 Å, slightly longer than that of rare Ti_2^+. The most stable structures of $\mathrm{Au}_n\mathrm{Ti}_2^+$ ($n \leqslant 5$) have the shortest Ti–Ti bond length and the maximal numbers of Ti–Au bond than the other low-lying energy structures. This trend is interrupted for larger size clusters. As for $\mathrm{Au}_6\mathrm{Ti}_2^+$ cluster, however, the 6-I has shorter Au–Ti distance, though 6-I have slightly larger Ti–Ti bond than 6-II. For the $\mathrm{Au}_7\mathrm{Ti}_2^+$, the most stable structure 7-I has one more Au–Au bond than 7-II (Fig. 1). It can be understood that the gold atoms will play a more and more important role in determining the structures of $\mathrm{Au}_n\mathrm{Ti}_2^+$ clusters as the cluster size increasing.

In Figure 2 (top), we present the second-order difference of total energies $E(n)$ defined by $\Delta_2 E = E(n+1) + E(n-1) - 2E(n)$, which is a sensitive quantity that characterizes relative stability of atomic clusters as a function of cluster size. A clear odd-even staggering and noticeable

Table 1. The average coordination number n, average first-neighbor Ti–Au distance, $d_{\mathrm{Au-Ti}}$ (Å), Ti–Ti distance, $d_{\mathrm{Ti-Ti}}$ (Å) and binding energy per atom, E_b (eV) of the few low energy isomers of cationic $Au_nTi_2^+$ clusters for ($n \leqslant 7$). The geometry notation is that of Figure 1.

System	n	$d_{\mathrm{Au-Ti}}$	$d_{\mathrm{Ti-Ti}}$	E_b
1-I	2	2.598	2.331	1.126
1-II	2	2.456		0.873
1-III	1	2.432	2.561	0.829
2-I	4	2.599	2.279	1.805
2-II	4	2.605	2.321	1.771
2-III	4	2.593	2.378	1.763
3-I	6	2.605	2.307	2.158
3-II	6	2.610	2.563	2.053
3-III	5	2.573	2.834	2.018
4-I	8	2.623	2.370	2.331
4-II	8	2.598	2.800	2.234
4-III	6	2.547	3.507	2.190
4-IV	6	2.547	3.220	2.136
5-I	10	2.647	2.421	2.499
5-II	10	2.567	2.689	2.337
5-III	7	2.525	3.363	2.274
5-IV	6	2.596		2.157
6-I	11	2.736	2.378	2.559
6-II	12	2.819	2.294	2.540
6-III	12	2.807	2.479	2.497
6-IV	10	2.613	2.467	2.479
7-I	12	2.687	2.488	2.650
7-II	12	2.677	2.506	2.633
7-III	13	2.809	2.414	2.585
7-IV	12	2.696	2.527	2.557

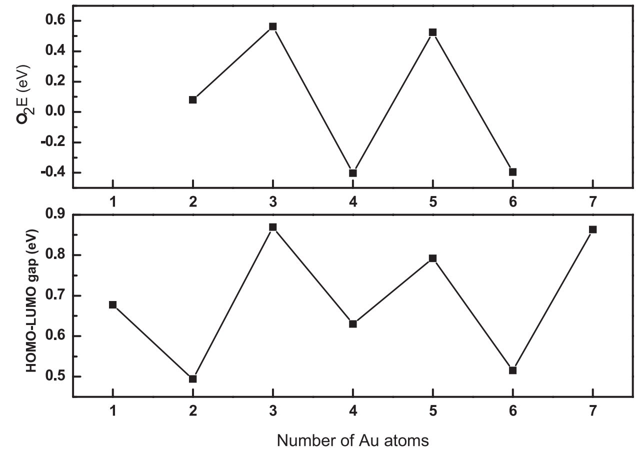

Fig. 2. (Top) Second-order energy differences ($\Delta_2 E$) and (bottom) HOMO-LUMO gap (eV) of the ground state versus number of gold atoms for $Au_nTi_2^+$ clusters.

Table 2. Positive charge on Ti_2 dimer and charge transfer (in a.u.), local magnetic moment on the Ti_2 of $Au_nTi_2^+$ clusters with ($n \leqslant 7$) and total magnetic moment (in μ_B), obtained from Mulliken population analysis.

Clusters	Charger	Charge transfer	Magnetic moment on Ti_2 (μ_B)	Total magnetic moment (μ_B)
$AuTi_2^+$	1.082	0.067	1.95	2.0
$Au_2Ti_2^+$	1.196	0.182	0.99	1.0
$Au_3Ti_2^+$	1.250	0.228	1.61	2.0
$Au_4Ti_2^+$	1.230	0.212	0.80	1.0
$Au_5Ti_2^+$	1.232	0.210	0	0
$Au_6Ti_2^+$	1.295	0.274	0.75	1.0
$Au_7Ti_2^+$	1.246	0.180	0	0

Table 3. The charge and magnetic moment of $3d$ and $4s$ states for per Ti atom of $Au_nTi_2^+$.

	$3d$		$4s$	
n	Charge	Magnetic moments	Charge	Magnetic moments
1	2.700	0.944	0.617	0.010
2	2.706	0.463	0.481	0.045
3	2.686	0.877	0.386	0.022
4	2.703	0.437	0.350	0.013
5	2.730	0.000	0.313	0.000
6	2.693	0.402	0.330	0.023
7	2.642	0.000	0.355	0.000

peaks for $\Delta_2 E$ at $n = 3$ and 5 are found. The peaks at $Au_3Ti_2^+$ and $Au_5Ti_2^+$ indicate that these clusters should be more stable than the clusters with neighboring sizes. The coincidence of pattern seen in $\Delta_2 E$ with the experimental abundance [20] indicates a good total energy calculation. The HOMO-LUMO gap presented in Figure 2 (bottom) also shows an odd-even staggering. It is currently believed that the higher the gap, the higher the cluster stability. Peaks in the HOMO-LUMO gap appear at the same n values already commented on for $\Delta_2 E$.

3.2 Charge and magnetic moment

We performed Mulliken population analysis for the lowest energy structures and the atomic charges of Ti dimer of the $Au_nTi_2^+$ are list in Table 2. One finds that the Ti_2 of $AuTi_2^+$ loses more than one electrons and there is a weak charge transfer from Ti_2 to Au atom. Starting from $n = 2$, the amount of charge on Ti_2 converges to a constant value. It does mean that the Ti_2^+ cation can form in the $Au_nTi_2^+$ clusters. Previous studies demonstrate that the charger of ionic Au_nM clusters are mainly distribute at the transition metal impurities [11,12,21]. And the charge has a significant effect on the magnetism of clusters.

Basing on the optimized geometries, we have calculated the magnetic properties of $Au_nTi_2^+$ clusters (results are shown in Tab. 2). We consider different spin states for multiplicity of the state. The ordering of the atomic magnetic moments for each spin state is given after calculation. For small $Au_nTi_2^+$ clusters with $n = 1$ to 4, the total magnetic moment shows a pronounced odd-even effect and is mainly located on the Ti_2^+ dimer. Small amount of spin is found on the Au atoms. However, larger $Au_nTi_2^+$ with $n = 5$ and 7 are completely nonmagnetic, whereas $Au_6Ti_2^+$ has a magnetic moment of $1.0\mu_B$. A detailed analysis of the atomic charge and the local magnetic moment is performed. The charge and spin of $3d$ and $4s$ orbitals for Ti atoms in $Au_nTi_2^+$ clusters are listed in Table 3. Obviously, the magnetic moment of the Ti atoms is mainly due

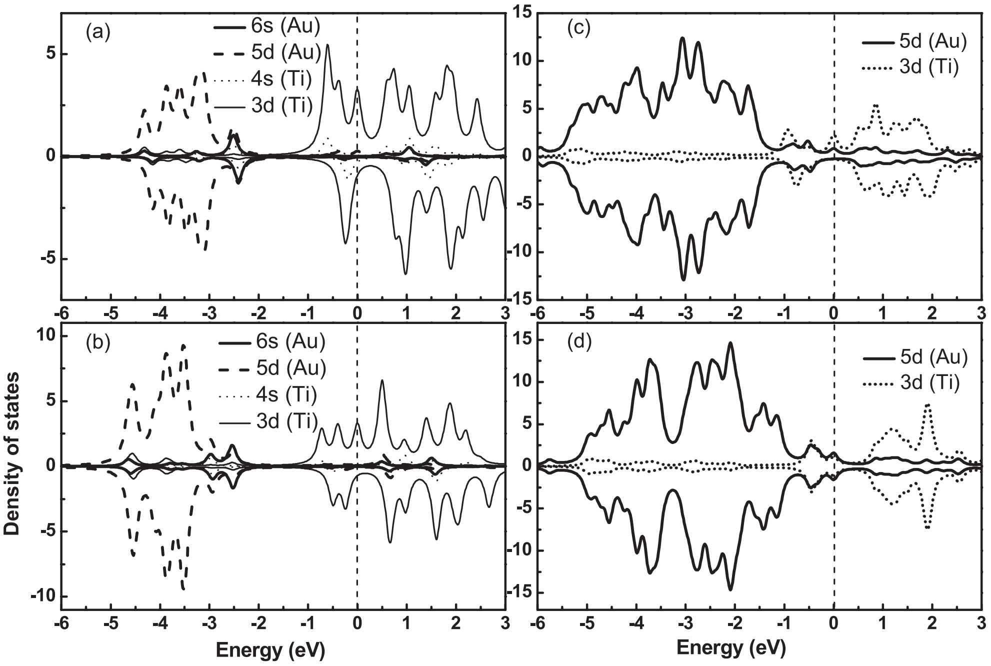

Fig. 3. The partial density of states (PDOS) of *s*, and *d* orbital for (a) AuTi_2^+; (b) $\mathrm{Au_2Ti}_2^+$; (c) $\mathrm{Au_6Ti}_2^+$; (d) $\mathrm{Au_7Ti}_2^+$; spin up (positive) and spin-down (negative) densities are given in each case. The dashed lines locate the HOMO.

to 3*d* electrons of Ti atoms. For free Ti atom, the ground-state electronic configuration is $3d^24s^2$. In the cases of $\mathrm{Au}_n\mathrm{Ti}_2^+$ clusters, the 3*d* state gain about 0.7 electrons, meanwhile the 4*s* state loses some amount of electrons. It suggests that there is a strong hybridization between 3*d* orbitals and 4*s* orbital of the titanium atoms, which has a remarkable influence on the magnetism of $\mathrm{Au}_n\mathrm{Ti}_2^+$ clusters.

It should be noted that there is a charge transfer from Ti atoms to Au atoms in $\mathrm{Au}_n\mathrm{Ti}_2^+$ (Tab. 3). And the charge transfer mainly happens between Ti 3*d*, 4*s* and Au 5*d*, 6*s* states, which indicates the Ti 3*d*, 4*s* orbitals hybridize with Au 5*d*, 6*s* orbitals. To explore the origin of peculiar magnetic properties, we show the partial density of states (PDOS) of Au 6*s*, 5*d* and Ti 3*d*, 4*s* orbitals for represented $\mathrm{Au}_n\mathrm{Ti}_2^+$ clusters in Figure 3. The spin-down density is plotted as negative. The Fermi level of cluster is presented as a dashed vertical line and shifted to zero. Despite a larger gap between the Au-5*d* band and the Ti-3*d* band is observed for small $\mathrm{Au}_n\mathrm{Ti}_2^+$ clusters with $n = 1$ and 2. However, there is a hybridization between the Ti 4*s* state and Au 5*d*, 6*s* states. For $\mathrm{Au_2Ti}_2^+$, the 4*s* state tend to deeper energy levels than in AuTi_2^+, which suggests that the interaction between Ti 4*s* orbital and Au 5*d*, 6*s* orbitals become stronger. As the size of cluster increasing, the Au-5*d* band is close to the Fermi level and overlaps with the Ti-3*d* band. These results imply that the hybridization between Ti 4*s*, 3*d* and Au 5*d* states might be one major reason for the peculiar magnetic properties. Previous studies have also shown that the magnetism of TM doped clusters is importantly influenced by the hybridization between the *s*, *d* orbitals of TM and host atoms [9,21–25]. On the other hand, the most stable structure of $\mathrm{Au}_n\mathrm{Ti}_2^+$ cluster can be obtained by adding a gold atom to that of $\mathrm{Au}_{n-1}\mathrm{Ti}_2^+$. As the addition of a gold atom, there is structural transition along with a significant change of magnetism. Comparing the DOS of $\mathrm{Au}_n\mathrm{Ti}_2^+$ and that of $\mathrm{Au}_{n+1}\mathrm{Ti}_2^+$, it can be clearly seen that the additional gold atom has a significant effect on the Ti-3*d* DOS (Fig. 3). Furthermore, the transition size for the formation of a pentagonal bipyramid structure with high symmetry is at $n = 5$. And the structure for $\mathrm{Au_7Ti}_2^+$ can be obtained by symmetrically adding two Au atoms to the pentagonal bi-pyramid structure. Thus, there might be some correlation between the geometry structure and the magnetic moment.

4 Conclusions

Using first-principles calculations, we investigate the atomic and electronic structure of cationic gold cluster doped with double titanium atoms, $\mathrm{Au}_n\mathrm{Ti}_2^+$. Tow titanium atoms form a dimer in the clusters and the bond length of the dimer is slightly changed as the cluster size increasing. Trends versus *n* of HOMO-LUMO gap, second-order energy differences of total energies, show these magic numbers and odd-even effects coincide with the experimental abundance. The magnetism as a function of $\mathrm{Au}_n\mathrm{Ti}_2^+$ cluster shows an odd-even effect and quenched at $n = 5$ and 7. Detailed analysis revealed that the structures and interactions of Ti 3*d*, 4*s* orbitals with Au 5*d*, 6*s* orbitals make important contribution to the magnetism.

One of the authors (Mingxing Chen) especially thanks Prof. X.G. Gong for helps. This work was supported by the Program for New Century Excellent Talents in University (Grant No. NCET-04-0779) and partly by the National Natural Science Foundation of China (Grant No. 10674070) and the Program for Changjiang Scholars and Innovative Research Team in University (Grant No. IRT0534).

References

1. W.D. Knight, K. Clemenger, W.A. de Heer, W.A. Saunders, M.Y. Chou, M.L. Cohen, Phys. Rev. Lett. **52**, 2141 (1984)
2. W.A. de Heer, Rev. Mod. Phys. **65**, 611 (1993)
3. M. Vogel, K. Hansen, A. Herlert, L. Schweikhard, Eur. Phys. J. D **16**, 73 (2001)
4. M. Sakurai, K. Watanabe, K. Sumiyama, K. Suzuki, J. Chem. Phys. **111**, 235 (1999)
5. P. Pyykkö, N. Runeberg, Angew. Chem., Int. Ed. **41**, 2174 (2002)
6. X. Li, B. Kiran, J. Li, H.J. Zhai, L.S. Wang, Angew. Chem., Int. Ed. **41**, 4786 (2002)
7. Y. Gao, S. Bulusu, X.C. Zeng, J. Am. Chem. Soc. **127**, 15680 (2005)
8. S. Neukermans, E. Janssens, H. Tanaka, R.E. Silverans, P. Lievens, Phys. Rev. Lett. **90**, 033401 (2003)
9. E. Janssens, S. Neukermans, H.M.T. Nguyen, M.T. Nguyen, P. Lievens, Phys. Rev. Lett. **94**, 113401 (2005)
10. E. Janssens, S. Neukermans, X. Wang, N. Veldeman, R.E. Silverans, P. Lievens, Eur. Phys. J. D **34**, 23 (2005)
11. M.B. Torres, E.M. Fernández, L.C. Balbás, Phys. Rev. B **71**, 155412 (2005)
12. E. Janssens, H. Tanaka, S. Neukermans, R.E. Silverans, P. Lievens, Phys. Rev. B **69**, 085402 (2004)
13. B. Delley, J. Chem. Phys. **92**, 508 (1990); DMol^3 is a DFT-based package with atomic basis, distributed by Accelrys, Inc. as a part of Materials Studio `http://www.accelrys.com`
14. J.P. Perdew, Y. Wang, Phys. Rev. B **45**, 13244 (1992)
15. A.V. Walker, J. Chem. Phys. **122**, 094310 (2005)
16. F. Remacle, E.S. Kryachko, J. Chem. Phys. **122**, 044304 (2005)
17. S. Gilb, P. Weis, F. Furche, R. Ahlrichs, M.M. Kappes, J. Chem. Phys. **116**, 4094 (2002)
18. S.H. Wei, Z. Zeng, J.Q. You, X.H. Yan, X.G. Gong, J. Chem. Phys. **113**, 11127 (2000)
19. T.K. Ghanty, K.R.S. Chandrakumar, S.K. Ghosh, J. Chem. Phys. **120**, 11363 (2005)
20. Y.-K. Han, J. Chem. Phys. **122**, 136101 (2005)
21. X. Li, B. Kiran, L.-F. Cui, L.-S. Wang, Phys. Rev. Lett. **95**, 25340 (2005)
22. S.Y. Wang, J.Z. Yu, H. Mizuseki, Q. Sun, C.Y. Wang, Y. Kawazoe, Phys. Rev. B **70**, 165413 (2004)
23. Q. Sun, X.G. Gong, Q.Q. Zheng, D.Y. Sun, G.H. Wang, Phys. Rev. B **54**, 10896 (1996)
24. D.W. Yuan, Yang Wang, Z. Zeng, J. Chem. Phys. **122**, 114310 (2005)
25. J. Wang, G. Wang, X. Chen, W. Lu, J. Zhao, Phys. Rev. B **66**, 014419 (2002)